Exploration of Iron ore deposits in Patagonia. Insights from gravity, magnetic and SP modelling

Rodolfo Christiansen[1*], José Kostadinoff [2], Julia Bouhier[2], Patricia Martinez[1]

[1] IGSV – CONICET - UNSJ - San Juan, Argentina

[2] Departamento de Física – UNS – Bahía Blanca, Argentina

*Corresponding author

E-mail: rodolfo.christiansen@conicet.gov.ar

Instituto Geofísico Sismológico Volponi - UNSJ

Ruta 12 - km 17. Marquesado, San Juan, Argentina. CP 5407

Phone / Fax: +54 9 264 4945015

ABSTRACT

The Sierra Grande region in northern Patagonia is considered the largest iron ore reserve in Argentina; however, the extension of the non-outcropping deposits as well as the depth of the basins that contain them remains unknown. Utilizing 3D litho-constrained inversion of

gravity and magnetic data, we delimited an area with good prospects for iron ore deposits. In this region, high resolution magnetic and self-potential profiles were acquired over the most important anomalies. Correlating both methodologies, it was possible to specify the possible existence of iron oxides (martite-hematite) in the form of 2D inclined sheets.

Keywords: Gravity, Interpretation, Inversion, Modelling

1 INTRODUCTION

The presence of iron ore deposits in the area of Sierra Grande in northern Patagonia Argentina has been studied since 1951. However, Pleistocene-Holocene sediments and volcanic rocks cover most of the region hindering their precise location and making it necessary to explore through indirect methods. In this region there are outcrops of the Sierra Grande Formation containing important economic iron ore deposits. Previous geophysical investigations determined a series of negative gravity anomalies that were interpreted as a succession of Paleozoic basins parallel to the Patagonian coast as a result of a probable Permian-Triassic extension. (Gregori *et al*., 2013, Gregori *et al*., 2016).

In order to expand the iron ore reserves, three geophysical techniques have been implemented: Gravity, magnetic and self-potential (SP). The combination of geophysical methods provides indirect information for the delimitation of ore bodies and have been widely used in mineral exploration. The reader can refer to Barnes and Romberg (1943), Hinze (1960), Martinez *et al.* (2010) to supplement their interest in historical cases of exploration of iron by means of potential methods. However, the combination of the SP method together with gravity and magnetic surveying techniques with the objective of iron exploration has not been published. Nevertheless, because of the high sulfide content in the

nearby deposits and the shallow depth of the bodies, it was considered a possible good method for this particular case (Burr, 1982; Heiland, 1940; Sato and Mooney, 1960).

2 GEOLOGICAL SETTING

The geology of the region under study (Figure 1) is the consequence of four major geotectonic events: Pampean, Famatinian, Patagonian and Andean.

The Pampean orogeny is represented by the oldest rocks and is constituted by metamorphic rocks grouped into two distinct units. The Mina Gonzalito Complex is composed of schists, amphibolites, limestones (amphibolite facies) and granitoids. The second unit is composed of low-grade metamorphic rocks (meta-greywackes to quartzite phyllites) and is called the El Jaguelito Formation.

The Famatinian cycle comprises igneous rocks of Ordovician age characterized by granitoids of the Plutonic Complex Punta Sierra, including the Arroyo Salado Granodiorite, Hiparsa Granite and Punta Sierra Granite (Gregori *et al*., 2013). In angular discordance over these rocks and those of the Pampean cycle lie the sedimentary rocks of the Early Devonian-Silurian Sierra Grande Formation characterized by the abundance of sandstones, which occur in sequences alternated with pelites and, subordinate, quartzites. Based on the lithological characteristics and fossiliferous content, this unit was divided into two members: a lower called San Carlos and another superior called Herrada (Zanettini, 1981). These platform environment rocks have oolithic hematite (Fe_2O_3) and magnetite (Fe_3O_4) content associated with apatite minerals with up to 3.4% of phosphates and up to 1% content of sulfide (Zanettini, 1999). Its outcrops are located in three main zones denominated Northern, Southern and Eastern outcrops which contain three exploitable iron deposits (Northern, Southern and Eastern deposits).

The rocks of the Patagonian cycle are located discordantly above the previous units and comprise the Marifil Complex. This unit of Late Triassic-Upper Jurassic age occupies most of the region and comprises extrusive (lavas, ignimbrites and tuffs) and intrusive facies (dykes and domes) locally interspersed with sedimentary chemical and epiclastic facies.

The lower section of the Andean event is represented by marine inflows and regressions, interrupted by the continental deposits of the Sarmiento Formation and by the basaltic Oligocene rocks of the Somún Curá Formation. Finally, in the upper section of the Andean cycle there are the Pliocene Patagonian rounds and Pleistocene-Holocene alluvial and colluvial deposits.

Figure 1

2.1 IRON LAYERS

In 1963 the existence of two iron horizons dominated in composition by hematite with subordinate magnetite was established, which were named Rosales and Alfaro by Zanettini (1981). The Rosales Horizon is located in the San Carlos Member. It is present in the northern and southern outcrops and is the one that is exploited in the Southern deposit of Sierra Grande. It is disposed in up to four layers interspersed with sterile sediments (sandstones, limolites, and quartzites). The maximum ores have a thickness of 8.65 m and ore grade of 57.4% Fe in the Northern deposit and 14 m with an ore grade of 54.8% Fe in the Southern deposit (Zanettini, 1981).

The Alfaro Horizon is situated in the Herrada Member. In the Northern deposit it is formed by 2 to 6 lenticular strata of little thickness, whereas to the south it comprises only two levels and constitutes

the Eastern and Southern deposits with a maximum exploitable thickness of 6.60 m and an ore grade of 51.2% Fe.

2.3 GEOLOGICAL STRUCTURES

The recognition of the structures becomes very difficult due to the coverage of Pleistocene-Holocene sediments in most of the area. The metamorphic units that constitute the basement were intensely folded by several diastrophic phases and they were intruded by granitoids of Ordovician age.

As regards the Sierra Grande Formation, its main structural features are folding and faulting. The anticlines and synclines are mostly closed, with axes oriented in varying azimuths between 315º and 355º, and of asymmetric character with east-verging axial planes (Zanettini, 1981).

The folding is affected by faults which have caused, in some cases, the exposure of the basement. These faults are generally N-S oriented with eastern and western vergence. A secondary faulting is recognized, represented by thrust faults, generally E-W oriented although it is also NW-SW oriented. It is considered that the rocks of the Sierra Grande Formation were affected by the Famatinian and Gondwanic deformation (Gregori *et al.,* 2013). The Patagonian rocks present tilts due to the first phases of the Andean Orogeny, whereas the deposits of the Upper Tertiary are not affected.

3 METHODS

The prospecting phase was carried out in a regional and local stage. In the first, gravimetric and magnetic data were acquired approximately every 1 km, although gravimetric data cover a larger area (see section 3.1 Regional Survey). The inversion of these anomalies is a

fundamental tool to establish the shape of the basin and areas with high susceptibilities (comparable with those produced by dikes with iron content) on a regional scale (see section 3.2 3D Litho-constrained Inversion). Once these data are interpreted, detailed exploration can be done in the most promising areas.

To assess the presence of iron sheets similar to those found in the vicinity of the area (Northern deposit), the study was complemented with high resolution profiles. The location of these was chosen based on the most significant magnetic anomalies and where the inversion model suggests the presence of materials with values of magnetic susceptibility of around 0.1 SI (see section 3.2 Local Survey). Over these lines, new magnetic stations every 12.5 m and SP sections using ($CuSO_4$) non-polarizable electrodes every 25 m were acquired. These data allow the construction of models in which the response of a generated geological model and the data obtained in the field can be compared. In this way the uncertainty in the location of the deposits covered by sediments is reduced.

3.1 REGIONAL SURVEY

Figure 2 shows the location of the acquisition of the geophysical data and the control profiles utilized in the inversion of gravity (red) and magnetic (blue) data. These were created in order to observe the geology model in different positions and depths. The theoretical gravity was calculated using the International Gravity Formula 1967 and referenced to the IGSN71 network of Argentina. The formulas proposed by Blakely (1995) were used to calculate the Bouguer gravity anomalies considering an average rock density of 2.67 g/cm^3 (Hinze, 2003). Terrain effects were subtracted by a combination of the method described by Nagy (1966) and Kane (1962) for the terrain density of 2.67 g/cm^3. On the other hand, Total Magnetic Anomalies (TMA) were calculated subtracting the International Geomagnetic Reference Field (IGRF) to the base corrected magnetic values.

Figure 2

The Bouguer anomalies contain the effects produced by all the bodies placed in the subsurface. Each of them provides a signal to the observed field, which results in complex overlapping anomalies (Nettleton, 1976). In our case, the structure of interest is located in the upper crust, where the sedimentary basin and possible mineral deposits of economic interest are situated. By subtracting a 3rd order trend surface from the observed gravity, the map of residual anomalies was obtained (Figures 3a, 3b, 3c).

As in the case of the gravity data, the residual TMA grid was obtained subtracting a 3rd order trend surface from the observed anomaly (Figures 3d, 3e, 3f). These data present great difficulty in its visual interpretation because of the asymmetry caused by the inclination and declination in the magnetic field. The Reduction to the Magnetic Pole method (RTP) was utilized to reconstruct the magnetic field at a 90° Inclination (I) and a zero Declination (D), thus locating the anomalies above the respective sources. However, being unable to know the true direction of magnetization, these could be distorted.

Figure 3

3.2 3D LITHO-CONSTRAINED INVERSION

The geophysical inversion method carried out in this paper was implemented using GeoModeller software developed by Intrepid Geophysics and BRGM (Calcagno et al., 2008;

Guillen et al., 2008). This method uses geological interfaces and orientation data to create a continuous 3D model to describe the geometry of the geology. Once this is achieved, gravity and magnetic data can be combined to adjust the limits and shapes of the different geological units under certain constrains. The result is a quantification of the lithology and the distribution of rock property in a probabilistic way.

Given the difference in the distribution of the data, and considering that the main geological units have low magnetic susceptibility, the inversion was calculated in two stages. In the first, only the gravimetric data was considered in order to obtain the shape of the basin. A 3D reference model consistent with all of the geological observations (location of the geological units, direction, dip) was constructed using geostatistical interpolation (Calcagno *et al.,* 2008). The initial density values and standard deviations were set according to the density values published by Gregori *et al.* (2008). For those that we did not have data, it was assigned by following international tables. The thickness of the Cenozoic sediment cover was set according to the information of the water wells in the region, which suggests a depth of 40 meters in the western sector and 100 meters in the central zone. The model was discretized into voxels of 500 x 500 x 100 m (x, y, z). Then, a forward computation was performed to ensure that the model was consistent with the potential field datasets.

The inversion algorithm uses a framework of geological units with the following constraints: Stratigraphic order, which indicates if the order of the stratigraphic column is preserved; Shape ratio, which compares how similar it is the actual surface area/volume from the initial; Commonality, which compares the initial cells with that of the proposed model; and Volume Ratio, which compares the proposed volume to the reference or initial volume.

An iterative inversion procedure (McInerney *et al.,* 2005) was used to generate several millions possible models. With each iteration, the starting litho-model, the density values and the inversion constraints were changed and evaluated. This procedure was carried out until reaching a good adjustment between the anomaly grids produced by the computed geology and the observed geophysical data. After several inversion runs, the most probable geological model for the area was obtained.

During the second stage, the previously obtained geology shapes were fixed and the magnetic susceptibility was inverted in a similar manner. This inversion was important to locate volumes where the susceptibility assumes values similar to those found in the actual deposits in the area, 0.1 SI for the iron layers (martite-hematite) and 0.02 SI for the metamorphic basement rocks. In this way the area where to carry out the local exploration was reduced.

3.3 LOCAL SURVEY

The regional data inversion provided density and susceptibility models allowing to select the most promising prospection areas. Thus, local magnetic data were acquired. Moreover, taking into account the inversion models and considering the low depth of the Paleozoic sedimentary rocks (less than 100 meters) and the content of sulfide of the mineral deposits, the self-potential method was considered as a useful exploration tool for this area (Heiland, 1940; Sato and Mooney, 1960).

Since the magnetic sources of interest (vertical tabular dikes) are approximately at a depth of 100 meters and no deeper than the basement, the new magnetic signals acquired on the profiles, which contain shallow and deep contributions, were filtered. To remove the regional

trend (long wavelength) the data were upward continued to a height of 250 m and the resultant values were subtracted from the original data. Then the noise (short wavelength) was removed by a low pass filter with a cut-off wavelength of 150 m (Hinze *et al.,* 2013).

The high resolution magnetic and the SP data were interpreted along 2 profiles. These data were modelled using the 2D Talwani's method (Talwani *et. al.,* 1959) on GM-Sys 2D modelling software assuming, in analogy with the nearby iron deposits, the presence of tabular dikes with a thickness of 4 and 9 m and high angle dips.

Several studies have shown the shapes of SP anomalies on profiles for inclined metal plates or the response to a series of sources (Adeyemi *et al*., 2006; Biswas and Sharma, 2014; Biswas *et al.,* 2014). Considering this, the tops of the dikes with vertical dips were located close to the minima of SP. Then the values of the magnetic susceptibility were obtained by a non-linear inversion process taking into account the amplitudes of the anomalies. Finally, the inclinations were modified until the anomalies generated by the model reproduced satisfactorily the observed magnetic data.

4 RESULTS

High amplitude gravity anomalies can be observed in the sector of the locality of Sierra Grande coinciding with outcrops of Pampean and Silurian-Devonian rocks suggesting the presence of a basement high (Figure 4 a)**.** Figure 4b shows the 3D model projected over 4 N-S control profiles (1, 2, 3, and 4 in Figures 2, 3, 4 and 5). The most probable geology was obtained according to the density distribution (Figure 4c). On the other hand, Figure 5 shows the original residual gravity grid, the resultant gravity grid produced by the inversion model

and the misfit between both of them. A very low misfit between the response of the model and the data obtained in the field was achieved.

Towards the north, there is a gravity minimum in the La Planicie zone represented by a circular anomaly of approximately 30 km in diameter. This result allows us to assure that this is the response of a basin of sedimentary rocks of lower density than the rocks of the basement. It should be noted that the edges of this gravity anomaly have very high gradients (see Figure 3e). The inversion model suggests that the depth of this basin is about 2000 m in average reaching in its deepest part 4000 m. To the south, two extensional basins (half grabens type) of approximately 2000 m of thickness can be observed, in which the Sierra Grande Formation would be covered by the volcanic rocks of the Marifil Formation.

Figure 4

Figure 5

Figure 6 shows the magnetic inversion of the La Planicie area. The most promising areas are located to the NW of the basin and are represented by high values of magnetic anomalies (Figure 3 f) although they are lower compared to those found in the Sierra Grande area. The inverted susceptibility shows values of around 0.1 SI for profiles LP2 and LP3 at a distance of approximately 10,000 m from the beginning of the profiles (Figure 6c), however, the spacing of the data does not allow a good resolution. Figure 7 shows the original residual magnetic grid, the resultant magnetic grid produced by the inversion model and the misfit

between both of them. As in the gravimetric case, a good fit between the response of the model and the field data was achieved

Figure 6

Figure 7

In figure 8 the reduction to the pole of the residual magnetic data of the area (Figure 3f) can be observed. Based on the visible magnetic highs in the reduced to the pole map and the accessibility of the place, the location of two high resolution magnetic profiles and SP sections were selected (Profile 1 and Profile 2 in figure 8).

Figure 8

The SP sections extend for approximately one kilometer each. Variations between positive and negative values are here interpreted assuming the presence of near vertical iron sheets. The magnetic profiles (Figure 9) are of exactly equal length. These were filtered to remove the high amplitude noise.

Figure 9

The modelled sections for the main anomalies (Figures 10 and 11) resulted in tabular dikes with dips between 60 and 80 degrees (northward for profile 1 and southward for profile 2) and thicknesses of 4 to 9 m with average susceptibilities of approximately 0.1 SI. The

variation of the latter could be due to the difference in the content of hematite and magnetite as it is known in the nearby deposits.

With respect to the depths of the lower extremes of the dikes, these are not entirely clear due to the inability of the methods to define the extent of these bodies with certainty. Regarding the SP values, the correspondence between the greater susceptibilities and the major changes from positive to negative in the SP values for both profiles is remarkable.

Figure 10

Figure 11

5 DISCUSSION

The gravity anomalies in the area of La Planicie have been interpreted as a mass deficit originated by a basin whose filling is estimated by the outcrops found in the south of this area (Zanettini, 1981; Zanettini, 1999; Weber, 1983) as Paleozoic (Silurian-Devonian) sedimentary rocks of the Sierra Grande Formation. Results suggest that this basin is a continuation of the Sierra Grande Basin located at 32km to the south of the working area and separated from it by a structural high in the basement that was also responsible for the exposure of the Sierra Grande Formation.

Horizons containing iron oxides are also present and composed principally of martite-hematite in the form of tabular dikes. This result is based on the knowledge of the magnetic susceptibility of the nearest iron outcrops, where measurements made in the Northern deposit of Sierra Grande gave an average value of 0.10150 SI, being this value very similar to those

found by inversion of the magnetic data. This fact also explains the lower values of amplitude in the magnetic anomalies when compared with those of the Southern and Eastern deposits which contain more magnetite. Due to the intense folding, the thicknesses of the dikes are of approximately 4 meters and dip with high angle in opposite directions. This suggests that the structure consists of an antiform with its axial plane oriented in SE to NE direction in which the top is eroded (Figure 12). An alternative geological model is the possibility of the existence of disseminated sulfide or amphibolite in the basement rocks, such as those found in the Gonzalito mine (23 km to the west). These could generate SP and magnetic signals according to their composition.

Figure 12

6 CONCLUSIONS

The gravity method has provided a more complete understanding of the Paleozoic basins in the coastal zone of Northern Patagonia, especially that of La Planicie, which has an area of approximately 500 km^2. The occurrence of magnetic anomalies is related to the existence of levels with content of iron oxides, which are comparable with those of the Sierra Grande Basin. The low amplitude magnetic anomalies values and their correlation with the values of self-potential permit us to infer the presence of martite-hematite. For these reasons, this deposit could be considered as an extension of the Northern deposit.

To reject the alternative model that proposes the presence of sulfides, it is suggested to perform exploratory drilling. More accurate subsurface information will facilitate the correction of the models.

7 ACKNOWLEDGEMENTS

The authors would like to acknowledge Marifil S.A and Departamento de Física (Universidad Nacional Del Sur) for covering the financial costs of this project. The authors would also like to acknowledge Intrepid Geophysics for the Geomodeller software academic license and Consejo Nacional de Investigaciones Científicas y Técnicas (CONICET) for their research grant.

8 CONFLICT OF INTEREST

It is an in-house publication and has no conflict of interest with any other person or organization.

9 REFERENCES

Adeyemi, A., Idornigie, A., and Olorunfemi, M. 2006. Spontaneous potential and electrical resistivity response modelling for a thick conductor. Journal of Applied Sciences Research, 2, 691-702.

Barnes, V. E., and Romberg, F. 1943. Gravity and magnetic observations on Iron Mountain magnetite deposit, Llano County, Texas. Geophysics, 8(1), 32-45.

Biswas, A., and Sharma, S. P. 2014. Optimization of self-potential interpretation of 2-D inclined sheet-type structures based on very fast simulated annealing and analysis of ambiguity. Journal of Applied Geophysics, 105, 235-247.

Biswas, A., Mandal, A., Sharma, S. P., and Mohanty, W. K. 2014. Delineation of subsurface structures using self-potential, gravity, and resistivity surveys from South Purulia Shear Zone, India: Implication to uranium mineralization. Interpretation, 2(2), T103-T110.

Blakely, R. 1995. Potential Theory in Gravity and Magnetic Application. 441 pp. Cambridge University Press. ISBN: 052141508X

Burr, S.V., 1982. A guide to prospecting by the self-potential method: Miscellaneous Paper 99, Ontario Geological Survey, 15 p

Busteros, A., Giacosa, R., Lema, H., and Zubia, M. 1998. Hoja Geológica 4166-IV, Sierra Grande, Provincia de Río Negro. Subsecretaría de Minería de la Nación, Boletín, 241.

Calcagno, P., Chilès, J. P., Courrioux, G., and Guillen, A. 2008. Geological modelling from field data and geological knowledge: Part I. Modelling method coupling 3D potential-field interpolation and geological rules. Physics of the Earth and Planetary Interiors, 171(1), 147-157.

Gregori, D. A., Kostadinoff, J., Strazzere, L., and Raniolo, A. 2008. Tectonic significance and consequences of the Gondwanide orogeny in northern Patagonia, Argentina. Gondwana Research, 14(3), 429-450.

Gregori, D. A., Kostadinoff, J., Alvarez, G., Raniolo, A., Strazzere, L., Martínez, J. C., and Barros, M. 2013. Preandean geological configuration of the eastern North Patagonian Massif, Argentina. Geoscience Frontiers, 4(6), 693-708.

Gregori, D. A., Saini-Eidukat, B., Benedini, L., Strazzere, L., Barros, M., and Kostadinoff, J. 2016. The Gondwana Orogeny in northern North Patagonian Massif: Evidences from the Caita Có granite, La Seña and Pangaré mylonites, Argentina. Geoscience Frontiers, 7(4), 621-638.

Guillen, A., Calcagno, P., Courrioux, G., Joly, A., & Ledru, P. 2008. Geological modelling from field data and geological knowledge: part II. Modelling validation using gravity and magnetic data inversion. Physics of the Earth and Planetary Interiors, 171(1-4), 158-169.

Heiland, CA 1940. Geophysical Exploration. Prentice Hall. NY

Hinze, W. J. 1960. Application of the gravity method to iron ore exploration. Economic Geology, 55(3), 465-484.

Hinze, W. J. 2003. Bouguer reduction density, why 2.67?. Geophysics, 68(5), 1559-1560.

Hinze, W. J., Von Frese, R. R., and Saad, A. H. 2013. Gravity and magnetic exploration: Principles, practices, and applications. Cambridge University Press.

Kane, M. F. 1962. A comprehensive system of terrain corrections using a digital computer. Geophysics, 27(4), 455-462.

Martinez, C., Li, Y., Krahenbuhl, R., and Braga, M. 2010. 3D Inversion of airborne gravity gradiometry for iron ore exploration in Brazil. In SEG Technical Program Expanded Abstracts (pp. 1753-1757). Society of Exploration Geophysicists.

McInerney, P., Guillen, A., Courrioux, G., Calcagno, P., and Lees, T., 2005. Building 3D geological models directly from data? A new approach applied to Broken Hill, Australia. Digital Mapping Techniques 2005 Workshop in Baton Rouge.

Nagy, D. 1966. The gravitational attraction of a right rectangular prism. Geophysics, 31(2), 362-371.

Nettleton, L. L. 1976. Gravity and magnetics in oil prospecting. McGraw-Hill Companies.

Sato, M., and Mooney, H. M. 1960. The electrochemical mechanism of sulfide self-potentials. Geophysics, 25(1), 226-249.

Talwani, M., Worzel, J. L., and Landisman, M. 1959. Rapid gravity computations for two-dimensional bodies with application to the Mendocino submarine fracture zone. Journal of geophysical research, 64(1), 49-59.

Weber, E. I. 1983. Descripción geológica de la Hoja 40 j, Cerro el Fuerte, Provincia de Rio Negro: carta geológico-económica de la República Argentina, escala 1: 200.000. Servicio Geológico Nacional.

Zanettini, J. C. 1981. La Formación Sierra Grande (Provincia de Río Negro). Revista de la Asociación Geológica Argentina, 36(2), 160-179.

Zanettini, J. C. M. 1999. Los depósitos ferríferos de Sierra Grande, Río Negro. Recursos minerales de la República Argentina. Instituto de Geología y recursos minerales. Servicio Geológico Minero Argentino (SEGEMAR), Anales, 35, 745-762.

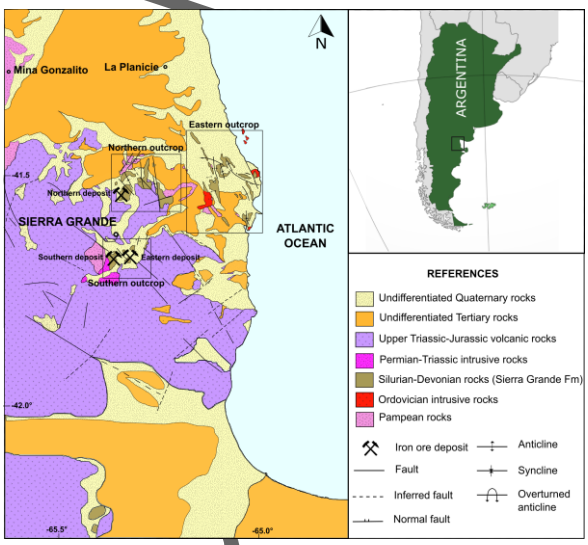

Figure 1. Simplified geological map of the area (Modified from Busteros *et al*. 1998). Black squares indicate the outcrops of the Sierra Grande Formation.

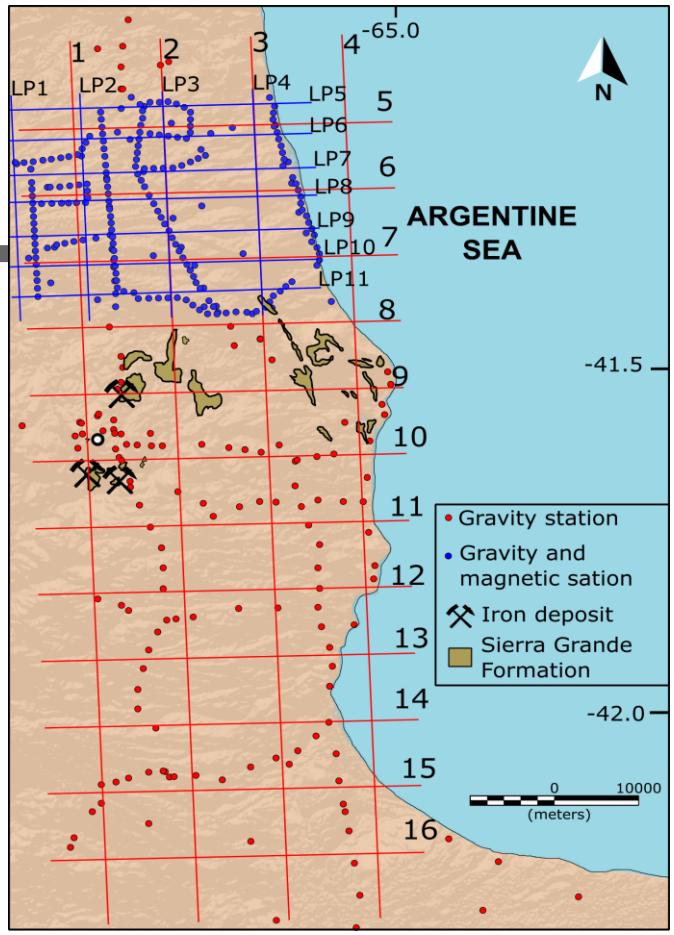

Figure 2. Gravity and magnetic measurements locations. Red circles: Gravity stations; Blue circles: Gravity and magnetic stations. Red lines: Gravity inversion control profiles. Blue lines: Magnetic inversion control profiles. In brown outcrops of the Sierra Grande Formation

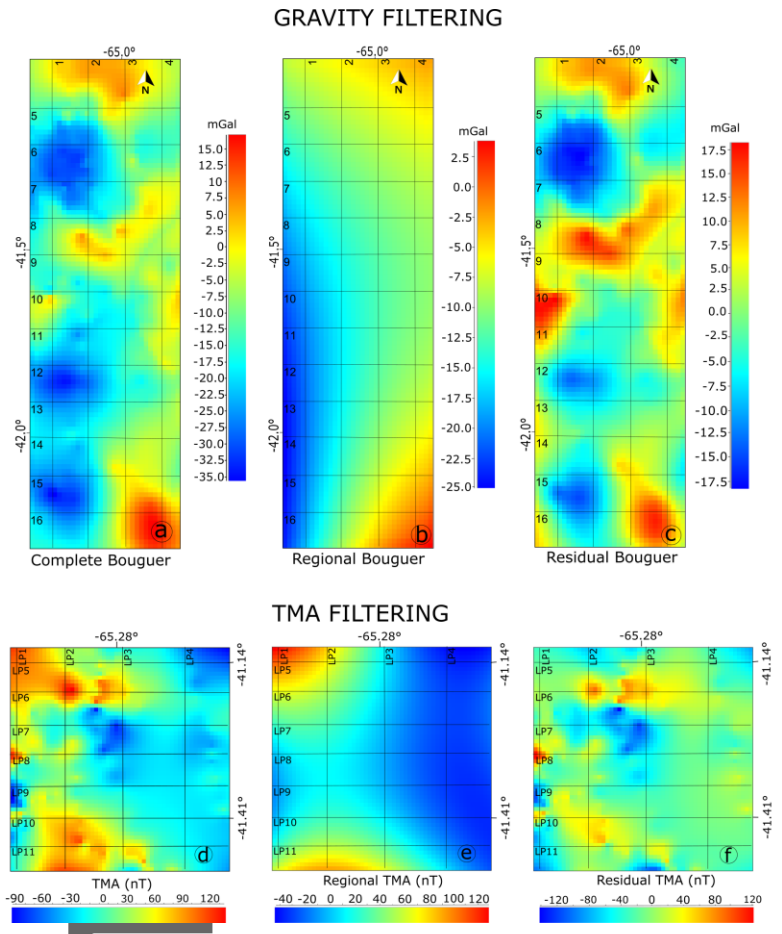

Figure 3. A 3rd order polynomial filter was applied to the Bouguer and TMA grids. a) Complete Bouguer Anomaly, b) Regional Bouguer Anomaly, c) Residual Bouguer Anomaly, d) TMA, e) Regional TMA, f) Residual TMA.

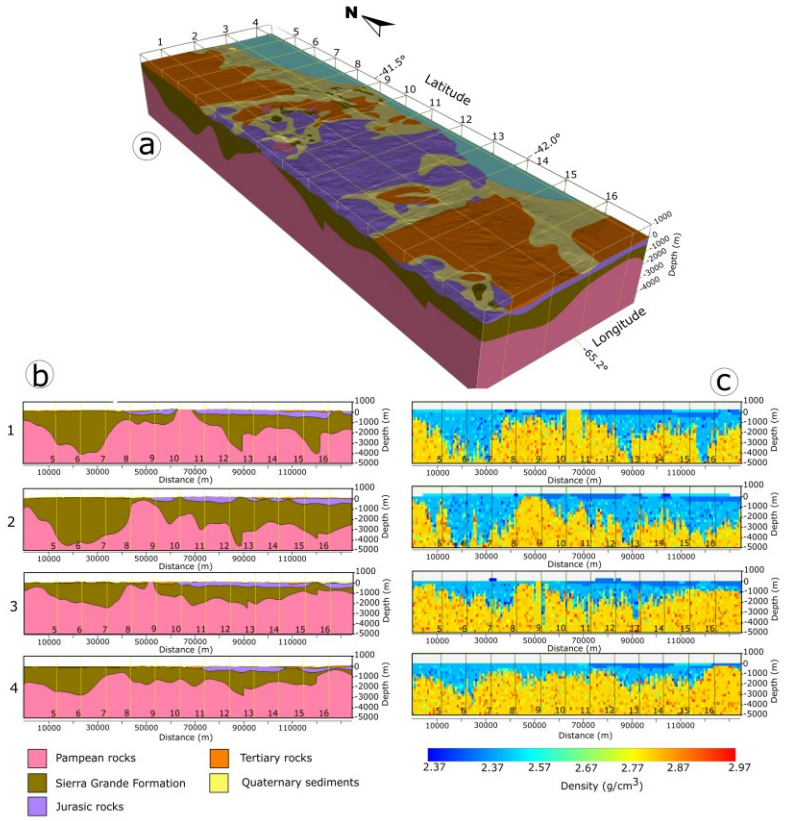

Figure 4. a) 3D geology model after gravimetric litho-constrained inversion. b) Most probable geology for control profiles in N-S direction. Due to the scale, the Tertiary and Quaternary formations are not seen in these sections. c) Density distribution of the control profiles

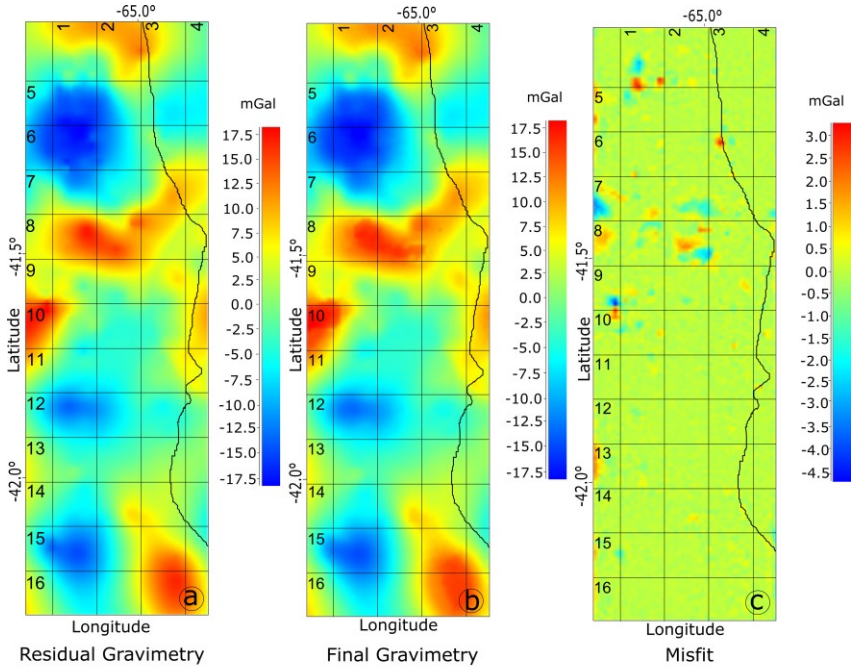

Figure 5. a) Residual gravity grid of the area. b) Gravity grid produced by the 3D inversion model (Figure 4) c) Misfit between the observed and the computed grids.

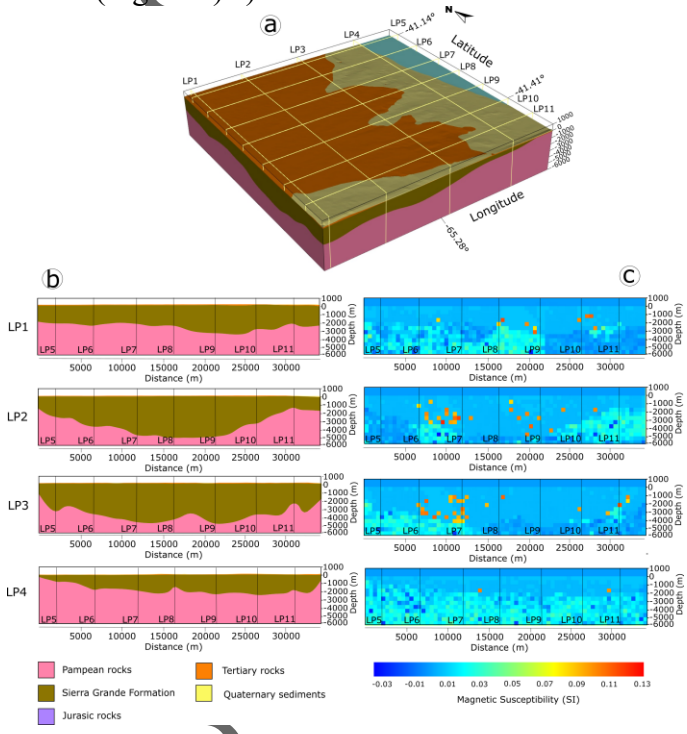

Figure 6. a) 3D geology model after magnetic litho-constrained inversion. b) Control profiles in N-S direction. c) Susceptibility distribution of the control profiles

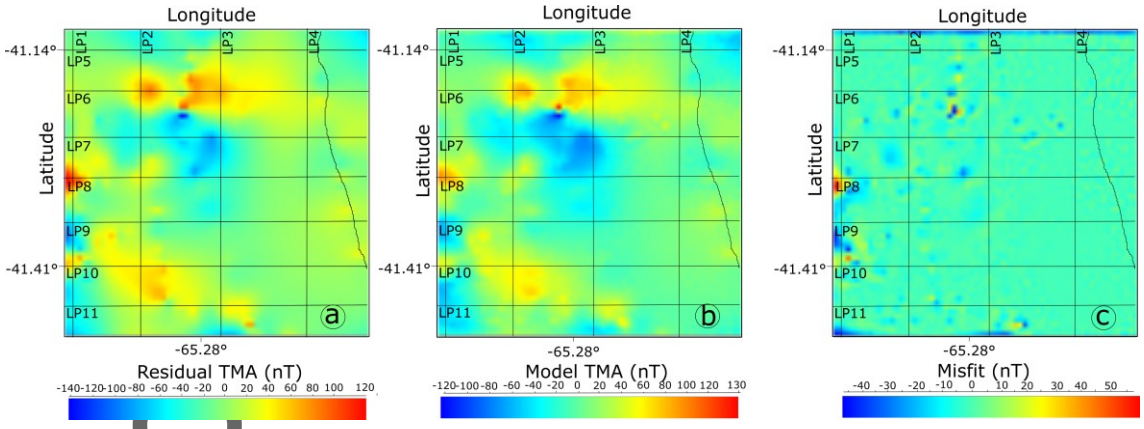

Figure 7. a) Residual TMA grid of the area. b) Magnetic grid produced by the 3D inversion model (Figure 6) c) Misfit between the observed and the computed grids.

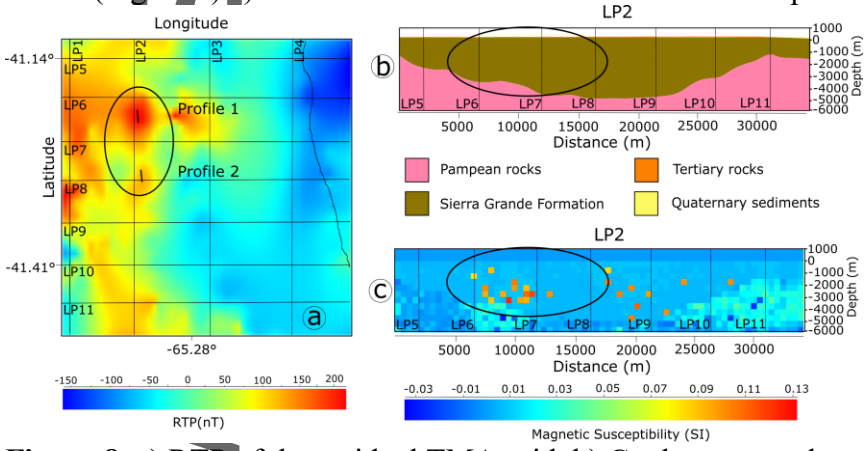

Figure 8. a) RTP of the residual TMA grid. b) Geology control profile LP2.
c) Susceptibility distribution of profile LP2

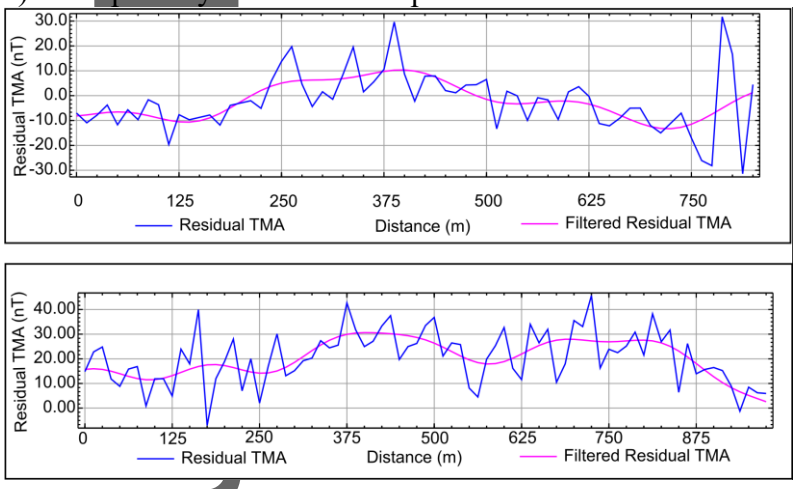

Figure 9. Magnetic profiles with stations every 12.5 m in lines concordant with those of SP (Location in Figure 8). Upper: Profile 1. Lower: Profile 2

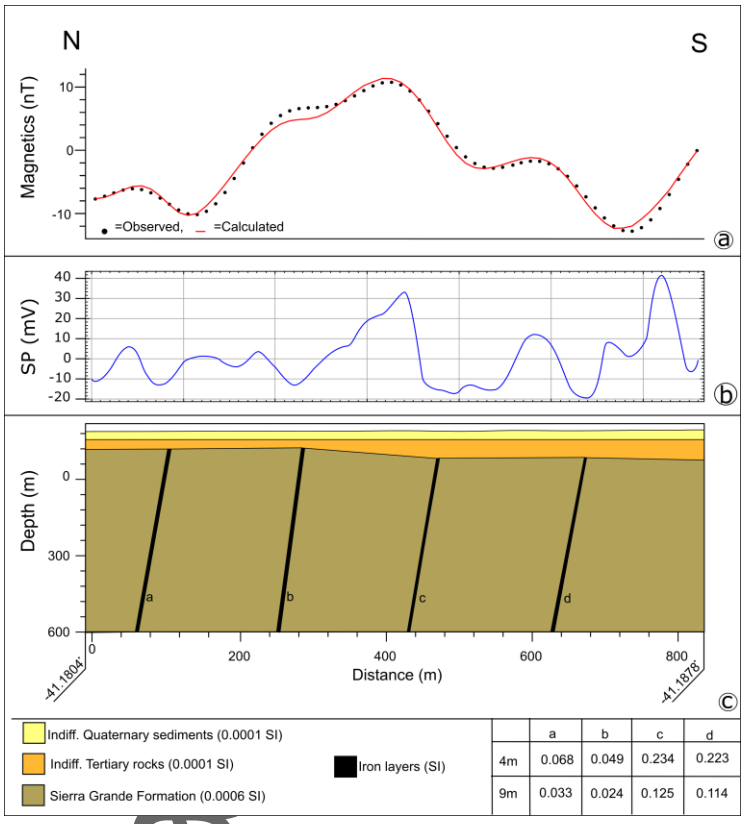

	a	b	c	d
4m	0.068	0.049	0.234	0.223
9m	0.033	0.024	0.125	0.114

Figure 10. Modelled section for profile 1 based on the filtered residual TMA and SP data. a) Magnetic data. b) SP data. c) Modelled geology.

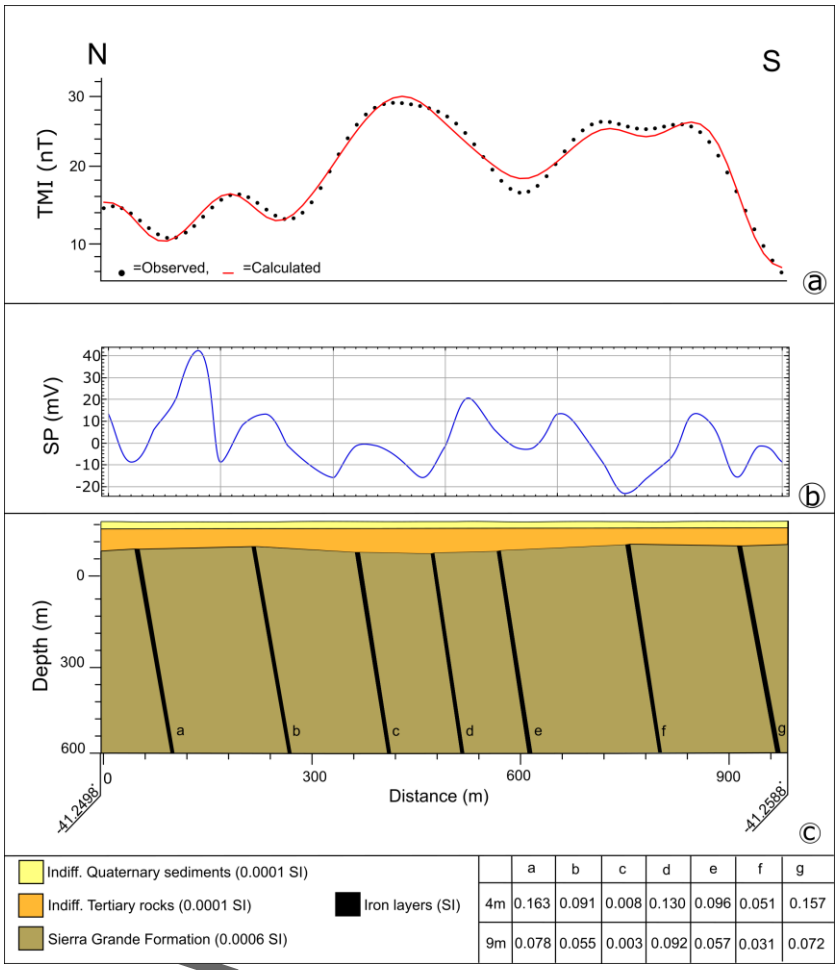

	a	b	c	d	e	f	g
4m	0.163	0.091	0.008	0.130	0.096	0.051	0.157
9m	0.078	0.055	0.003	0.092	0.057	0.031	0.072

Figure 11. Modelled section for profile 2 based on the filtered residual TMA and SP data. a) Magnetic data. b) SP data. c) Modelled geology.

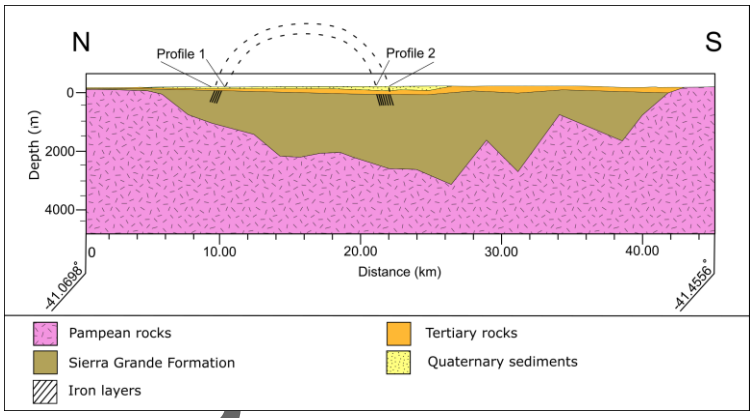

Figure 12. Schematic section for La Planicie Basin based on the residual gravity and SP anomalies.